

# Heavy Ion Results from ATLAS and CMS

**David Krofcheck**

The University of Auckland  
For the CMS and ATLAS Collaborations

d.krofcheck@auckland.ac.nz

**Abstract.** The heavy-ion programmes in the ATLAS and CMS experiments at the Large Hadron Collider aim to probe and characterise properties of the quark-gluon plasma created in relativistic nuclear collisions. This work presents selected results of collective effects, system size effects, and quarkonia production in p-p, p-Pb, Pb-Pb, and Xe-Xe collisions.

## 1. Introduction

The ATLAS[1] and CMS Collaborations[1] perform measurements in heavy ion (HI) collision programmes, in addition to proton-proton (p-p) discovery physics. The goal of the HI programmes is to discover and explain the properties of Quark-Gluon Plasma (QGP) created in these collisions. Smaller system sizes are also studied as cases in which QGP creation is not favoured. Recent results from Pb-Pb at centre-of-mass energies of 2.76 TeV and 5.02 TeV, Xe-Xe at 5.44 TeV, and p-Pb at 8.16 TeV are presented. Both HI programmes use p-p reactions as reference collisions to explore initial-state and final-state collision effects.

## 2. Collision System Size Effects

Most of the current HI programme uses the Pb-Pb system to probe hot and dense matter nuclear. More recent measurements are used to explore the Xe-Xe reaction, which provides a tool for exploring system size dependence on the production of hadrons.

### 2.1 Pb-Pb and Xe-Xe

Figure 1 shows the pseudorapidity density ( $dN_{ch}/d\eta$ ) of charged hadrons produced in nuclear collisions as a function of rapidity ( $y$ ) at different energies-per-nucleon [2]. The plot shows the expected growth in charged hadron production as both the LHC centre-of-mass energy increases, and the size of the collision region increases when going from Xe-Xe- to Pb-Pb reactions.



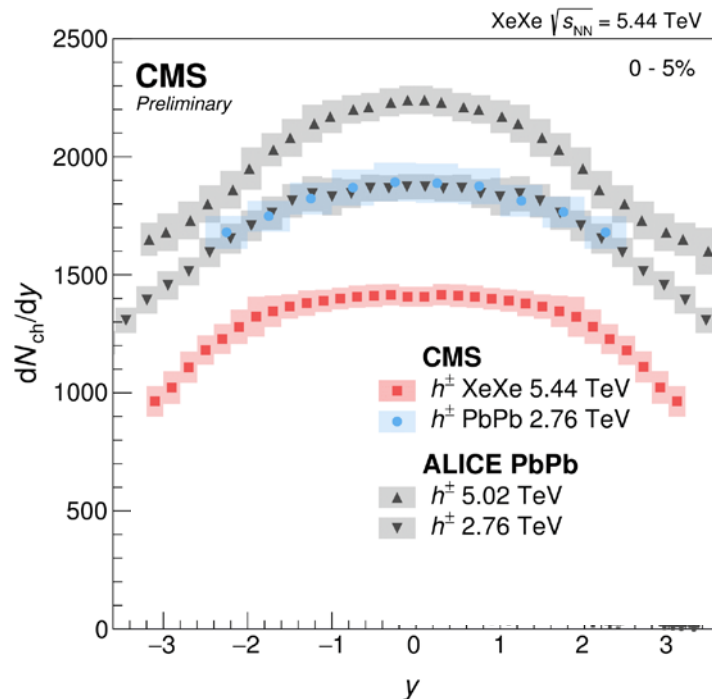


**Figure 1.** Average and symmetrised  $dN_{ch}/dy$  as a function of rapidity [2].

## 2.2 System size scaling

A study of the number of hadronic particles produced as a function of the average number of participants ( $\langle N_{part} \rangle$ ) is shown on the left side of Figure 2, for both Pb-Pb and Xe-Xe collisions. For fixed and large  $\langle N_{part} \rangle$  no system size scaling is observed.

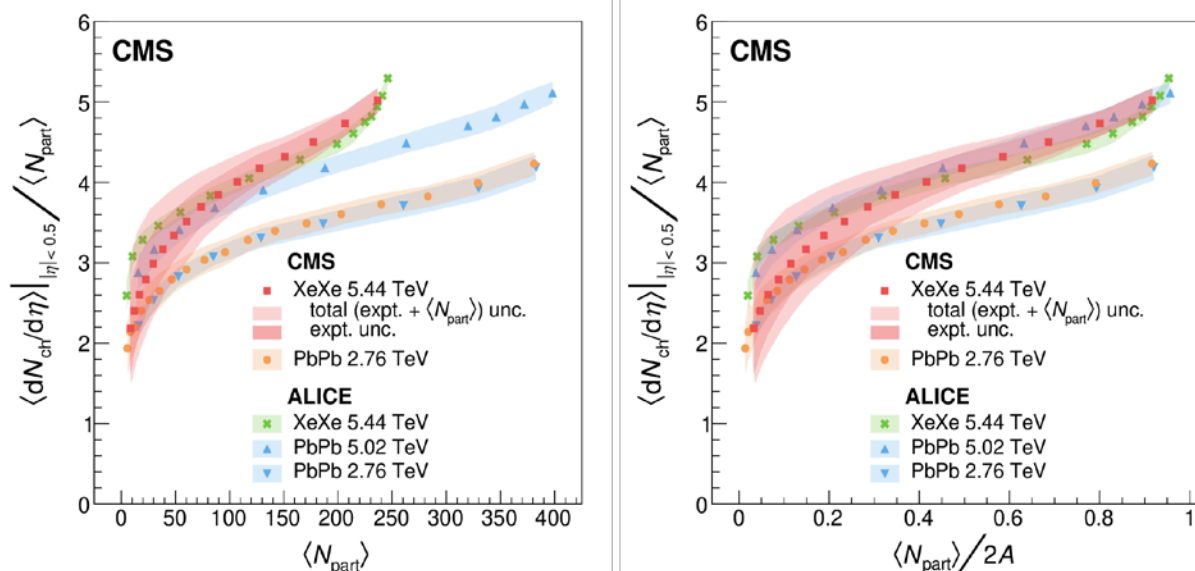


**Figure 2.** Average  $dN_{ch}/d\eta$  at mid-pseudorapidity ( $\eta$ ) normalised by  $\langle N_{part} \rangle$ , shown as a function of  $\langle N_{part} \rangle$  (left), and  $\langle N_{part} \rangle / 2A$  (right), where  $A$  is the atomic number of the nuclei [2].

The per-participant multiplicity for Xe-Xe and Pb-Pb collisions for the same  $\langle N_{part} \rangle$  and similar energies but different geometry or centrality are different. This is particularly evident for the most central (largest  $\langle N_{part} \rangle$ ) collisions. However, as in Figure 2 (right), where  $\langle N_{part} \rangle / 2A$  is used as a

substitute for centrality, the per-participant charged-hadron multiplicity for different colliding nuclei are equal within uncertainties when the geometry (centrality) and the energy of the compared systems are the same [2].

### 2.3 Charged particle suppression

Measurement of the nuclear suppression factor  $R_{AA}$  indicates how the QGP suppresses the observed charged hadron particle production. The data in Figure 3 show similar numbers of  $\langle N_{part} \rangle$  but for different centralities in the Xe-Xe and Pb-Pb systems. The Xe-Xe system exhibits slightly stronger suppression in the most central collisions.

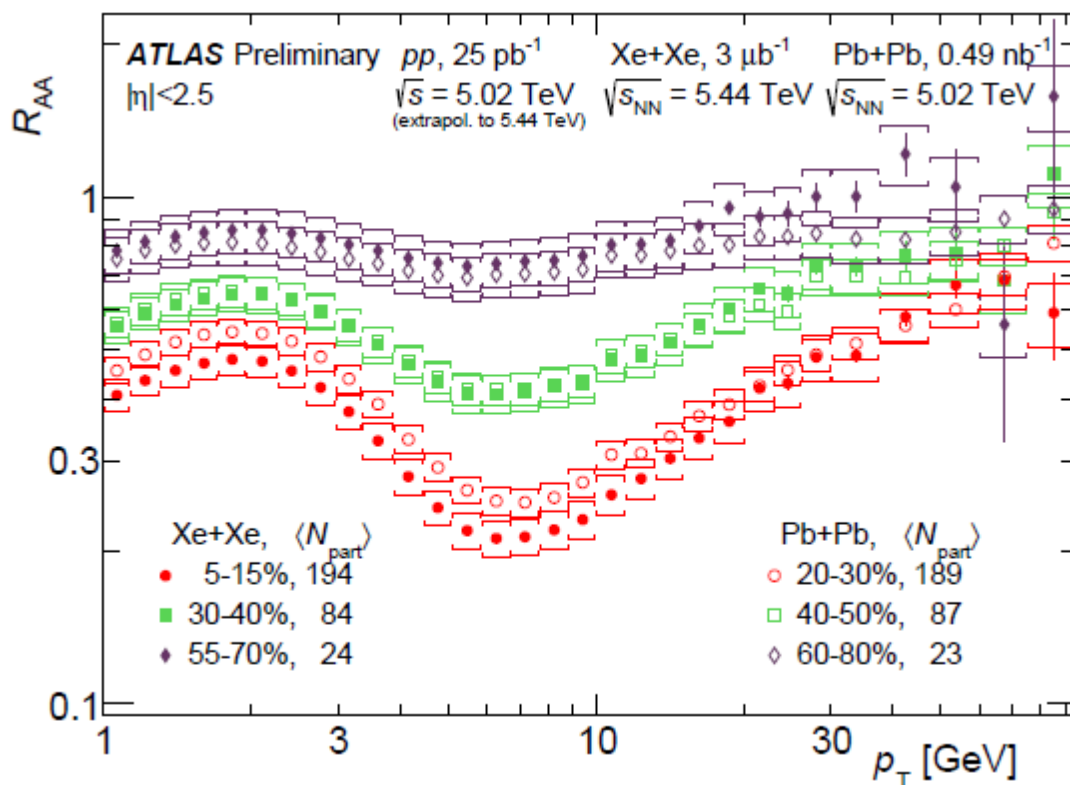


**Figure 3.** The nuclear modification factor  $R_{AA}$  for Xe-Xe and Pb-Pb systems [3].

## 3. Collective effects

Strong collective flow behaviour is exhibited in high energy nucleus-nucleus collisions. Studies of smaller systems such as p-Pb collisions and high multiplicity p-p collisions also reveal collective flow. Current research is aimed at measuring the flow of heavy quarks in small systems.

### 3.1 Charm and strange quark elliptic flow

In Figure 4 the background corrected  $V_2$ , called  $V_2^{\text{sub}}$ , per constituent quark for mesons and baryons is presented. For particle transverse kinetic energy per constituent quark values less than 1 GeV, the  $V_2^{\text{sub}}$  of prompt  $J/\psi$  mesons is consistent with prompt  $D^0$ ,  $K_S^0$  and  $\Lambda$  scaling along with the  $D^0$  meson. There is a suggestion of prompt  $J/\psi$  mesons, which consist of two charm quarks, breaking the scaling at higher

transverse kinetic energies. This is a hint that heavy quarks show weaker collective behavior in compressed nuclear matter.

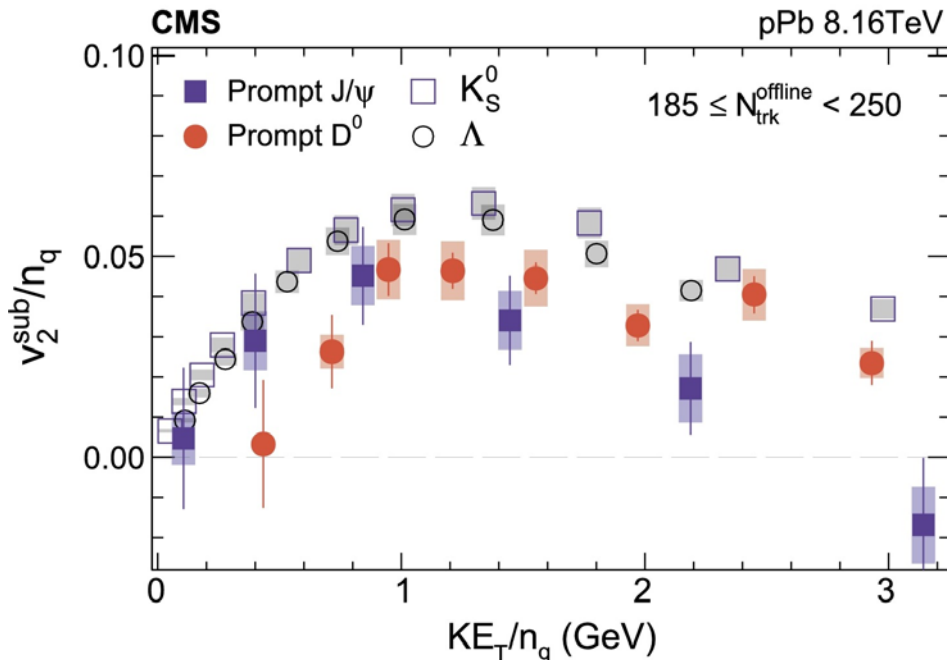


**Figure 4.** Background subtracted constituent quark normalized elliptic flow ( $V_2^{\text{sub}}/n_q$ ) as a function of normalized traverse kinetic energy [4].

### 3.2 Multiparticle correlations in azimuthal distributions

Multiparticle azimuthal correlations produced in heavy ion collisions extend over a considerable range in pseudorapidity. The observed azimuthal correlations are characterized by Fourier harmonics, with  $V_2$  and  $V_3$  referred to as elliptic and triangular flow, respectively [5]. The ratio between the four-particle and two-particle harmonics provides information on the relative importance of the global geometry and the fluctuation-driven asymmetries.

The first ever small system four-particle measurements of  $V_3$  are shown in Figure 5. For the small system formed in p-Pb (left side of Figure 5) the four-particle and two-particle harmonics are very similar. This is consistent with the origin of these harmonics coming from the same initial state fluctuation. For the larger system Pb-Pb (right side of Figure 5) the elliptic flow harmonic ratio is larger than the triangular flow harmonic. This result is expected if the global collision geometry dominates the Pb-Pb results [5].

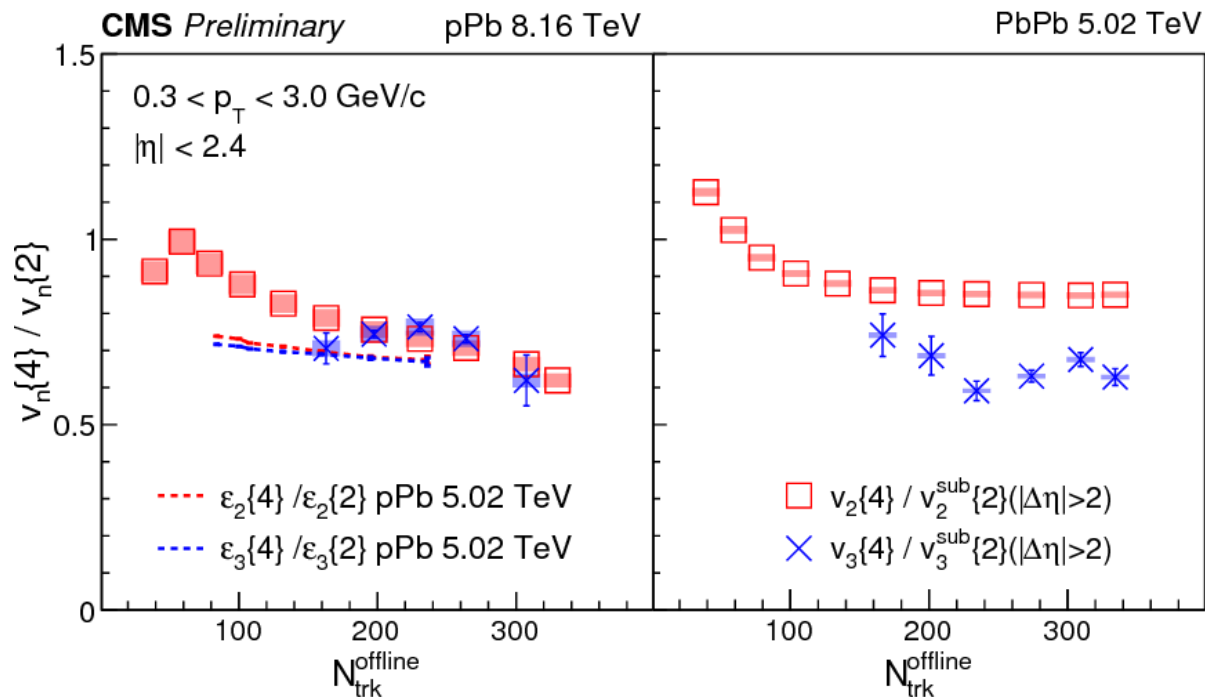


**Figure 5.** The ratios of four- and two-particle harmonics for pPb at 8.16 TeV (left), and for PbPb at 5.02 TeV (right) [5].

### 3.3 Dijet asymmetry

Dijets are sprays of particles produced in nucleus-nucleus collisions. If the dijets are approximately back-to-back then the phenomenon of jet quenching, the difference between the transverse energies of the two jets, can be observed.

New results on the dijet asymmetry (defined as  $X_J = P_T^2 / P_T^1$ , in which  $P_T^1$  is the leading jet transverse momentum, and  $P_T^2$  is the sub-leading jet transverse momentum) for Xe-Xe and Pb-Pb collisions are presented across four centrality bins in Figure 6 [3]. There appears to be very little difference in the behaviour of  $X_J$  as the size of the nuclear overlap changes. The jet quenching is uniform for central (0-10%) collisions and potentially evolves smoothly towards a non-uniform shape in the most peripheral (60-80%) collisions.

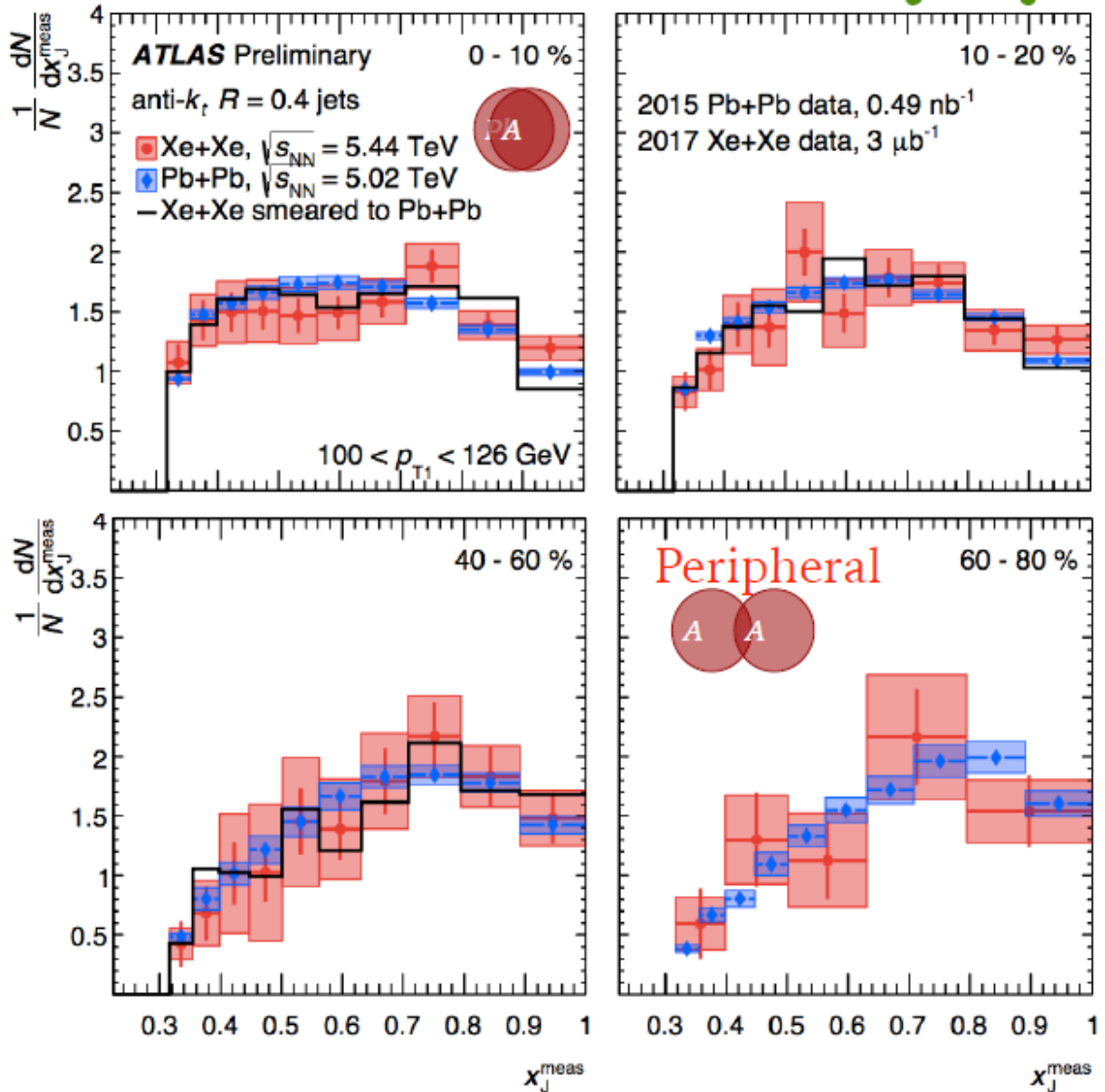


**Figure 6.** The normalised dijet asymmetry  $X_J$  in Xe-Xe and Pb-Pb collisions for four centrality bins [3].

Photons act as calibration probes in HI collisions as they essentially lose no energy as they traverse the QGP. One of the jets can be replaced by a high energy gamma ray. When comparing p-p collisions to Pb-Pb collisions the jet-gamma asymmetry parameter (defined as  $X_{J\gamma} = P_T^{\text{jet}}/P_T^\gamma$ ) behaves in a substantially different way than  $X_J$  defined for Figure 6. The  $X_{J\gamma}$  parameter for p-p reactions is compared to two centrality choices in Pb-Pb collisions at 5.02 TeV in Figure 7. Since the gamma-ray balances the jet momentum in p-p reactions we see a prominent peak at  $X_{J\gamma} = 1$ . In the Pb-Pb collisions we see a similar peak in peripheral collisions, but this peak smoothly evolves with increasing centrality. It nearly disappears for the most central (0-10%) Pb-Pb collisions. The jet momentum is quenched by the QGP in the central Pb-Pb collisions.

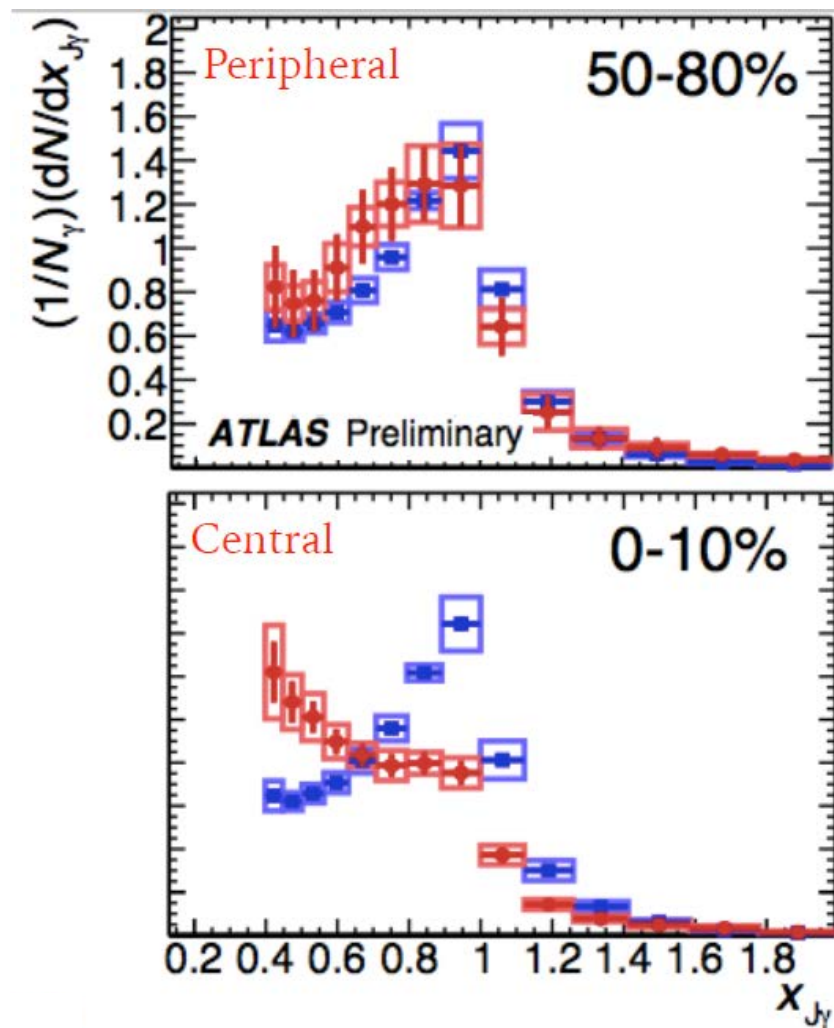


**Figure 7.** The jet-gamma asymmetry  $X_{J\gamma}$  in p-p and Pb-Pb collisions at 5.02 TeV for two centrality bins [6].

#### 4. Quarkonia and heavy quarks

Quarkonia and heavy quarks are also useful probes of QGP produced in HI collisions. The relevant observable quantity is the nuclear suppression factor ( $R_{AA}$ ). The  $J/\psi$  meson is composed of charm and anti-charm quarks. As shown in Figure 8, suppression of  $J/\psi$  production in Pb-Pb collisions gets larger as the collision centrality increases, e.g., more QGP is produced in the most central collisions (0-10%).

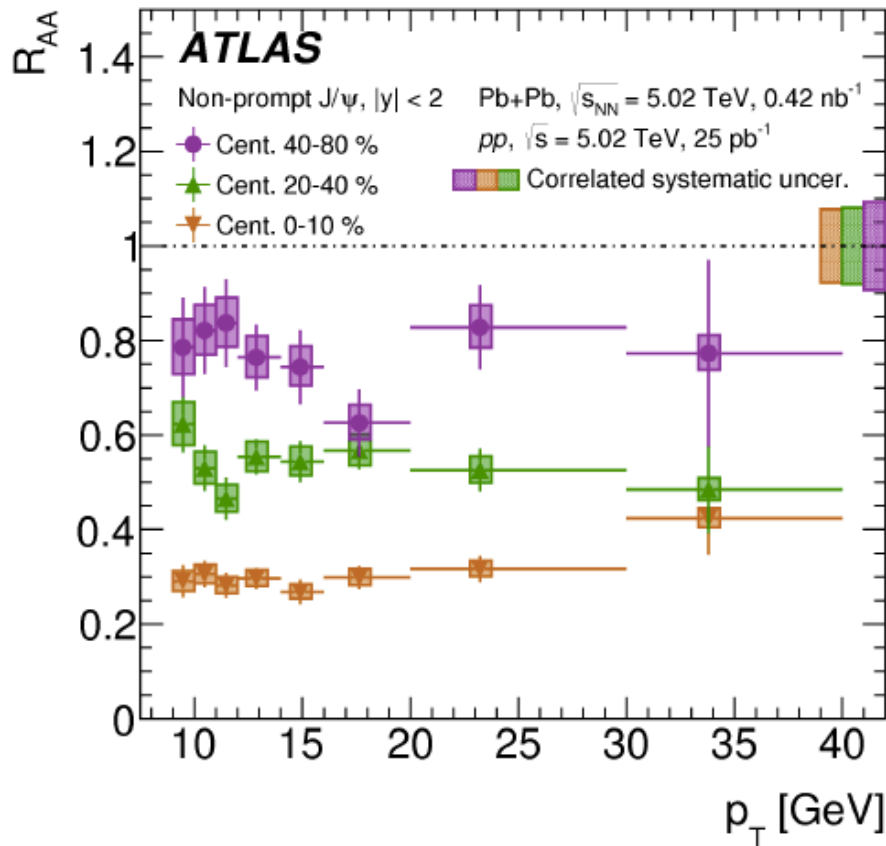


**Figure 8.** The nuclear modification factor  $R_{AA}$  as a function of  $p_T$  for prompt  $J/\psi$  production in Pb-Pb collisions at 5.02 TeV, shown for three centrality bins [7].

The  $J/\psi$  meson has an excited state called the  $\psi(2S)$ . The less tightly bound  $\psi(2S)$  is more sensitive to the high temperature QGP. This is illustrated in Figure 9 (left) where the  $R_{AA}$  is plotted for both the  $J/\psi$  and  $\psi(2S)$  mesons, as a function of participant particles in the Pb-Pb collision [8]. Prompt  $\psi(2S)$  are suppressed uniformly across the number of participants when compared to prompt  $J/\psi$  in Pb-Pb collisions at 5.02 TeV.

On the right side of Figure 9 is presented the nuclear suppression factor  $R_{pPb}$  for the p-Pb collisions at 5.02 TeV. p-Pb collisions are used to observe final state interactions. The  $\psi(2S)$  is expected to be suppressed by the same amount as the  $J/\psi$  meson, but the data in the negative rapidity region suggests that the  $\psi(2S)$  is more suppressed [8]. This may be due to the larger size of the  $\psi(2S)$  meson.

The  $\Upsilon$  meson also has a third excited state accessible in HI collisions. These mesons are labelled  $\Upsilon(1S)$ ,  $\Upsilon(2S)$ , and  $\Upsilon(3S)$  in Figure 10 [9]. Similar to the  $J/\psi$  meson and the  $\psi(2S)$  the three upsilon mesons, consisting of bottom and anti-bottom quarks, show a sequential suppression that increases as the collision centrality increases. The  $\Upsilon(3S)$  has the smallest  $R_{AA}$  observed for any hadron. Superimposed upon the data are ideal fluid hydrodynamics calculations [9].

Strangeness enhancement in HI collisions is accompanied by heavy quark creation. This motivates the search for strange neutral B mesons; e.g.,  $B_S^0 \rightarrow J/\psi \phi \rightarrow \mu^+ \mu^- K^+ K^-$  in A-A collisions. In Figure 11 (left) is an invariant mass yield plot of  $B_S^0$  mesons [10]. In Figure 11 (right) is the nuclear suppression  $R_{AA}$  for B mesons, with and without a strange quark, moving through QGP. Within current uncertainties, the results are consistent with models of strangeness enhancement and a suppression as observed for the  $B^+$  mesons.



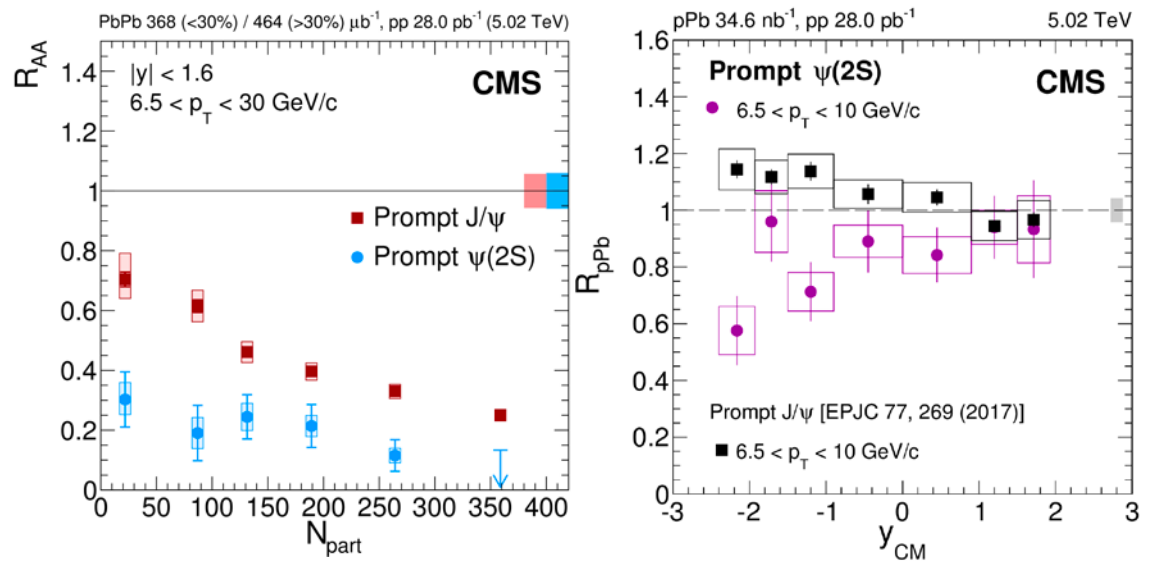


**Figure 9.** Nuclear suppression factors  $R_{AA}$  for  $J/\psi$  and  $\psi(2S)$  mesons in Pb-Pb(left) and in p-Pb (right) collisions plotted versus the number of participating particles ( $N_{part}$ ), and the rapidity ( $y_{CM}$ ), respectively [8].

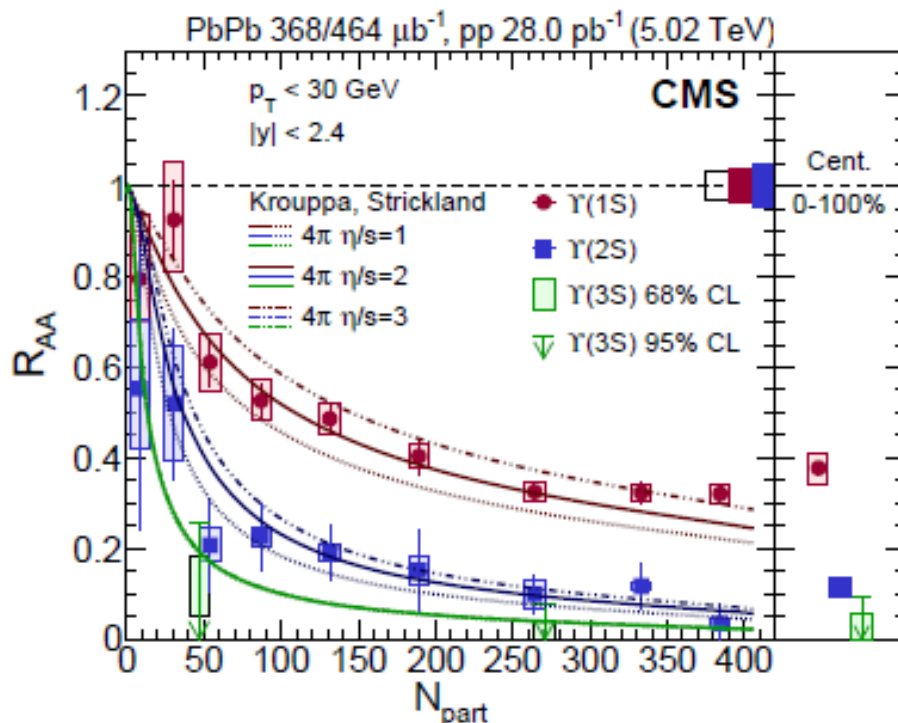


**Figure 10.** The nuclear modification factor  $R_{AA}$  as a function of  $p_T$  for  $Y(1S)$ ,  $Y(2S)$ , and  $Y(3S)$  production in Pb-Pb collisions at 5.02 TeV, shown as a function of the number of participating nucleons [9]. Ideal fluid model calculations by Krouppa and Strickland are also presented [9].

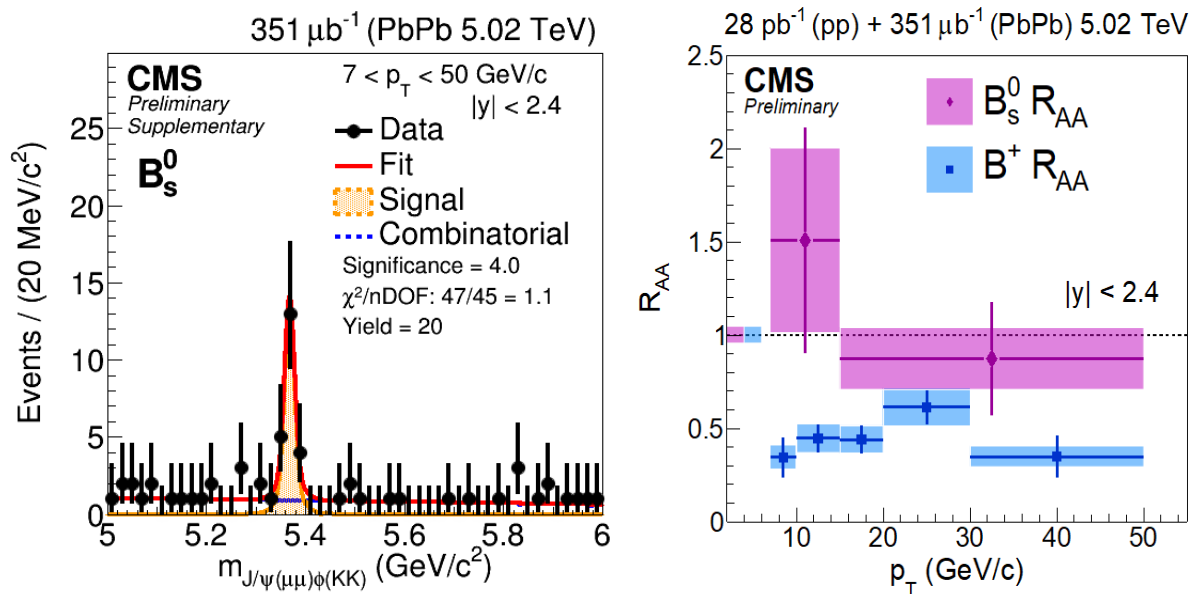


**Figure 11.** The invariant mass distribution for  $B_S^0$  decay in Pb-Pb collisions (left). Nuclear suppression factor for B mesons from Pb-Pb collisions (right) [10].

## 5. Conclusions

The heavy ion reaction programmes at both ATLAS and CMS are focussed on the study of QGP. A variety of particles and observables are used to investigate the earliest stages of nucleus-nucleus collision. System size effects, particle correlations, jet quenching, quarkonia, and heavy quark nuclear suppression provide insight to the earliest moments in relativistic nucleus-nucleus collisions.

## References

- [1] ATLAS Collaboration, *JINST* **3** (2008) S08003. <https://doi.org/10.1088/1748-0221/3/08/S08003>  
CMS Collaboration, *JINST* **3** (2008) S08003 <https://doi.org/10.1088/1748-0221/3/08/S08004>
- [2] CMS Collaboration 2019 (preprint <http://arxiv.org/abs/1902.03603>)  
*JHEP* **08** (2011) 141, [http://dx.doi.org/10.1007/JHEP08\(2011\)141](http://dx.doi.org/10.1007/JHEP08(2011)141)  
ALICE Collaboration <http://dx.doi.org/10.1103/PhysRevLett.106.032301>  
<http://dx.doi.org/10.1103/PhysRevLett.116.222302>
- [3] ATLAS Collaboration, (ATLAS-CONF-2018-007)
- [4] CMS Collaboration, 2019, *Phys. Lett.* **B 791**, 172 doi:10.1016/j.physletb.2019.02.018
- [5] CMS Collaboration, 2018 (CMS PAS HIN-17-004)
- [6] ATLAS Collaboration, (ATLAS-CONF-2018-009)
- [7] ATLAS Collaboration, 2018 *Eur. Phys. J.* **C78**, 762 doi:10.1140/epjc/s10052-018-6219-9
- [8] CMS Collaboration, 2018 *Eur. Phys. J.* **C78**, 509 [10.1140/epjc/s10052-018-5950-6](https://doi.org/10.1140/epjc/s10052-018-5950-6)  
CMS Collaboration, 2019 *Phys. Lett.* **B790** 509 [10.1016/j.physletb.2019.01.058](https://doi.org/10.1016/j.physletb.2019.01.058)
- [9] B. Kroupa and M. Strickland, 2016 Predictions for Bottomonia Suppression in 5.023 TeV Pb-Pb Collisions, *Universe* **2**(3) <https://doi.org/10.3390/universe2030016>  
CMS Collaboration, 2019 *Phys. Lett.* **B790** 270 <https://doi.org/10.1016/j.physletb.2019.01.006>
- [10] CMS Collaboration, 2018 (preprint <https://arxiv.org/abs/1810.03022>)  
CMS Collaboration, 2017 *Phys. Rev. Lett* **119** 152301  
<https://doi.org/10.1103/PhysRevLett.119.152301>